Journal of Applied Sciences

ISSN 1812-5654

science alert

ANSInet
an open access publisher
http://ansinet.com

Journal of Applied Sciences 13 (18): 3684-3690, 2013
ISSN 1812-5654 / DOI: 10.3923/jas.2013.3684.3690

Research on Siplification and Extraction Technology of Apple Point Cloud

[1,2]Hui-jun Yang, [1]Dong-jian He, [3]Shao-Hua Jiang and [2]Hua Wang
[1]College of Mechanical and Electronic Engineering, Northwest A and F University, Yang ling, Shaan xi, China
[2]College of Infortion Engineering, Northwest A and F University, Yang ling, Shaan xi, China
[3]Institute of Image Recognition and Computer Vision, Hunan Normal University, Changsha, Hunan, China

Abstract: Expensive computation, low efficiency and inaccuracy remain a long-standing challenge in extraction of fruit shape from massive background points. Towards these objectives, an improved K-neighborhood adaptive subdivision algorithm is proposed to simplify point clouds for reduction of calculation; an MLS-based local surface fitting is employed for more accurate geometric attributes and a Geometric Similarity-based Augmenter (GSA) recursive process is used for rapid extraction of apple shape. As a result, the optimal subdivision parameters help to reduce the number of apple cells to 3.0% of the original points, a 25% down than the K (4%) neighborhood, the GSA extraction algorithm reduce the number of extracted pear cells by 49.5%.

Key words: Apple splat, subdivision, simplification, extraction, MLS

INTRODUCTION

Since, the 3D scanner was developed by researchers, rich details can be acquired from scanned data with dense point clouds, without management of topological connection (Colombo *et al*., 2006), 3D scanners have been popularly used for information acquisition in various applications, including human face reconstruction (Zhou *et al*., 2008), architecture reconstruction (Nan *et al*., 2010) and tree construction (Vincent and Harja, 2008). Thus in fruit shape reconstruction, the data structure and algorithm are more simplified than tranditional mesh representation (Dong *et al*., 2003), image processing (Jancsok *et al*., 2001) and Finite Element Method (FEM) simulation (Uyar and Erdogdu, 2009).

While during the process of scanning apple in the fields, the point clouds from 3D scanner include stems, leaves, trunks and other background due to the apples are often grown on outdoor trees which make classical technology unavailable for apple shape reconstruction in agriculture. In order to enter the follow-up steps of registration, reconstruction and texture synthesis, points set simplification and accurate apple shape extraction from the background has become an important topic in reconstruction. In this study, apple shape extraction methods from scattered point cloud will be explored.

The great progress of our algorithm is that: At first, point octree is used for adaptive subdivision at arbitrary split positions by taking normals consistency into account to improving the K-neighborhood subdivision algorithm; then, each splat is locally approximated by MLS rather than circle or ellipse for more accurate geometric attributes and less gap between neighbor splats; at last, we present a recursive process based on Geometric Similarity Augmenter (GSA) to extract the "pure" apple splats from background.

The study is organized as follows, Section 2 describes the simplification and extraction algorithms; Section 3 gives simulation results of the algorithm on the 11 apple scans; Section 4 concludes this study and discusses future works.

ALGORITHM DESCRIPTION

Point clouds of apple scanned by laser scanners are a set of 3D points with laser intensity information in Eq. 1:

$$R = \{x_i, y_i, z_i\} \ (i = 1, 2...M) \quad (1)$$

It is set of unorganized 3D points with no topological relationship among them. Due to the drawback of existing methods on large amount of points, complicated calculation process and features obvious, this study puts forward geometric shape extraction algorithms by integrating simplification, local fitting and recursive GSA-based extraction on apple points set R. Ultimately,

Corresponding Author: Dong-jian He, College of Mechanical and Electronic Engineering, Northwest A and F University, Yang ling, Shaan xi, China

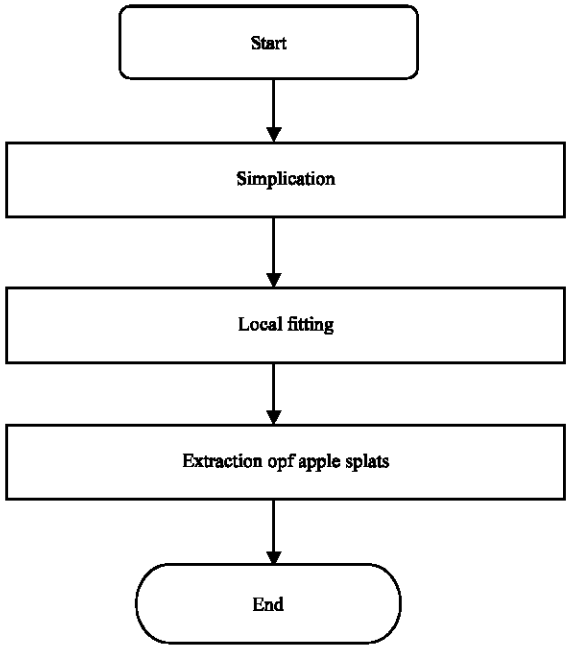

Fig. 1: Pipeline of extraction algorithm

the extracted subset is geometrical significance points set, i.e. a piece of complete apple scan. The pipeline of this step is shown in Fig. 1.

Simplification of point cloud: In view of the inadequate segmentation or over-segmentation of existing bottom-up K neighborhood on nonuniform curvature distribution surfaces of apple, this study improves K neighborhood by integrating point octree (Gross and Pfister, 2007) into apple point cloud R to produce top-bottom adaptive subdivision, shown in Fig. 2. So, the Simplification is a process to divide the points set into discrete hierarchical octree cells along an arbitrary axis inside the cell taht geometric features can be calculated for every cell.

In this study, the subdivision begins from a 3D closure which encloses the entire data space of apple point cloud R and max level n. According to the point distribution, each internal cell containing data is recursively decomposed into eight uncrossed and compactly supported subspace P_j. This process terminates if stopping conditions are satisfied, thus forming the data bucket of this cell $B_j = \{p_{j,1},..., p_{j,2}\}$ storing attributes of cells, such as, the center in Eq. 2:

$$\hat{p}_j = 1/m \sum_{i=1}^{m} p_{ji}$$

The radius in Eq. 3:

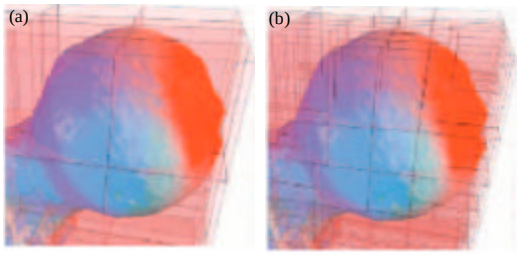

Fig. 2: Adaptive point octree partition at arbitrary positions

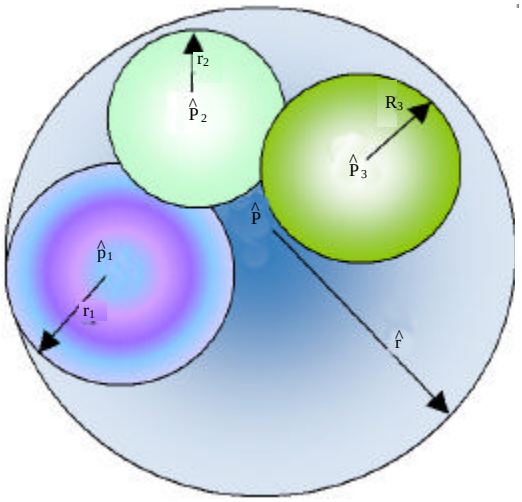

Fig. 3: Illustration of a bounding sphere

$$\hat{r}_j = \max_j (|\hat{p}_j - p_{ji}| + r_{ji}) \quad (3)$$

The radius of child node shown in Fig. 3. The normals of each point in Eq. 4:

$$n_{j,k} = (p_{j,k} - p_{j,k-1}) \times (p_{j,k+1} - p_{j,k}) \quad (4)$$

In the end, the recursive top-down algorithm is used for adaptive octree subdivision of apple scans by taking advantage of each cell's attributes. A cell is no longer divided when the number of points in a cell is less than a prespecified threshold k or normals characteristic of its points is consistency, as in Eq. 5:

$$\min\langle n_{ji}.n_{jk}\rangle > \delta \; \|n_{ji}\| = \|n_{jk}\| = 1 \quad (5)$$

The pseudo-code of algorithm is shown in Fig. 4.

Local splat fitting: In order to simplify the data structure, the aforesaid cells are converted to splats by approximating every cell with MLS surface for fitting the fruit local shape because each splat may have many

```
Octree(R) loop
 {
    If |R|≤k or Test_normal(n_ji,n_jk), then
       invoking Leaf_node(R) and put it into
 bucket
    initial P_j= Ø (j=0... ...7)
    p_split←Get_split_position(R)
    for i =1 to|R | //classify the point into 8
       j←Get_octant_code(p_split, p_i)
       P_j←P_j∪p_i
    For i =0 to 7 //records the non-null set
  if Pi≠Ø then
          ci←Octree(Pi)
 return New_octree_node(psplit, c0...7)
 }
```

Fig. 4: Pseudo-code of point octree subdivision

points and various curvatures. In general, splat was a counterpart of point taht is, point was first extended to splat one to one by circular or elliptical to fill the gaps between the samples (Gross and Pfister, 2007), thus the number of splats in a octree node is as many as that of points, so it's not fit to the fruit shape because of computational complication and various curvature in each splat.

While, in the Point Set Surface (PSS) theory, Moving Least Squares (MLS)-based PSS description is more stable in the local fitting on curvature various surface (Levin, 2003). And in first step, we obtained splat set P_j (j = 1, 2……N), each stores a bucket of data points $B_j = \{p_{j,1},..., p_{j,m}\}$, its center $\hat{p}_j$, radius $\hat{r}_j$ and normal n_j, N-the number of splats in splat set. So, in the study, a MLS-based surface S_j is proposed for defining splat P_j by a two-step projection operation which projects the point to the MLS surface (Wu *et al*., 2005).

In first projection, a tangent reference plane H_p is computed at the sphere center $\hat{p}_j$, is projected onto S_j and needn't be restricted to pass through H_p, shown in Eq. 6:

$$H_p = \{x|\langle n, x\rangle - D = 0, \|n\| = 1\} \quad (6)$$

Yet, the distance based influence of its neighbor points $\{p_{j,1},\ldots p_j\}$ to the origin of the tangent frame, is weighted by making the non-linear energy function minimum. This weight is called a partition of unity in Eq. 7:

$$\sum_{i=1}^{m}(\langle n, p_{j,i}\rangle - D)^2\theta(\|p_{j,i} - q\|) \quad (7)$$

Here, n-the normals of H_p, D-the distance from coordinate origin to H_p, θ (•)-Gaussian weight function in Eq. 8:

$$\theta(d) = e^{-d^2/(pa)^2} \quad (8)$$

In second projection, by weighted least square of all points in P_j on H_p, a local bivariate polynomials G_p is fitted with the coefficients being computed by minimizing the weighted least squares error in Eq. 9:

$$\sum_{i=1}^{m}(G_r(x_i, y_i) - h_i)^2\theta(\|p_j, i - q\|)$$

Here, (x_i, y_i)--the representation of p_{ij} in coordinate system of H_p, h_i--the height of p_{ij} over H_p.

Finally, curvature c_j is given in Eq. 10:

$$c_j = \lambda_1/(\lambda_1+\lambda_2+\lambda_3) \quad (10)$$

Here, λ_1-eigenvalues of the covariance matrix in Eq. 11 (Li, 2003):

$$(M)_j = \sum_{i=j}^{m}(p_{j,i} - \hat{p}_j)\times(p_{j,i} - \hat{p}_j) \quad (11)$$

So far, each splat has 4 properties, they are center $\hat{p}_j$, normals n_j radius $\hat{r}_j$ and curvature c_j which will be used for apple shape extraction in the following step.

Extraction of apple shape: Finally, accurate apple shape extraction has become a key step by in reconstruction. In state of the art, Marin *et al*. (2001) proposed a contribution to the "reverse engineering"-a method for the extraction of characteristic edges detected with a prior paraboloid fitting; Pang and Pang (2009) described a vision system that can extract such 2D/3D visual properties of mango as size, projected area, volume and surface area from multiple view images of mango; Wu and Meng (2008) proposed a robust object segmentation method; Iskurt and Becerikli (2010) developed a fast and automatic brain extraction by geodesic passive contour. The common features of all these extraction methods are that there was a foreseeable specific geometric shape to be extracted. While in our task, the fruit shape is random, so a recursive process is proposed for apple shape extraction by taking the splats basic selection and culling units.

In this study, a GSA-based iterative process is employed to generate pure apple splat sets, the curvature c_j and normals n_j are used to evaluate geometric similarity between splats. In initialization, the algorithm selects a seed splat P_k as base set, stack S as temporary memory, the Oct (splat) of octree leaf nodes as the ultimate splats storage, $flag_j$ of all leaf splats as 0 and the P_k is added to Oct (splat) (Wang *et al*., 2006), pushed to the stack S and set $flag_k$ = 1, show in Fig. 5a. When the stack is not empty, repeat the follow three-step:

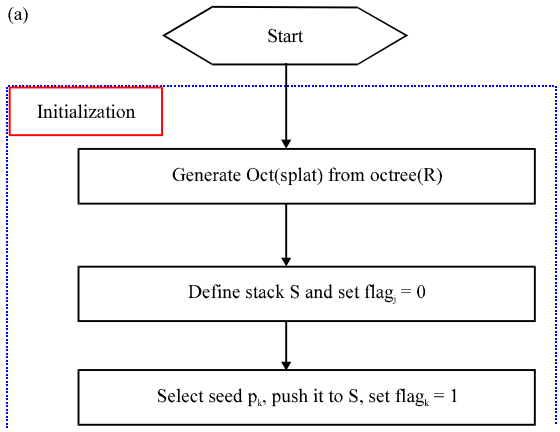

(b)
```
Oct(splat) loop
{
 If (S is not empty) then
 {        Pop splat p_k from S
          Search 8-neighbour p_i of p_k
          for i =1 to|8| // loop for 8-neighbours of p_i
          { if (satisfy||p_i-p_k||and flag_i=0) then
                    Push p_i to S, store p_i to Oct(splat)
                    set flag_i=1 }
 }
 Else
      end
}
```

Fig.5(a-b): Pipeline of extracting a set of apple splats (a) Initialization and (b) Pseudo-code of GSA-based iterative process

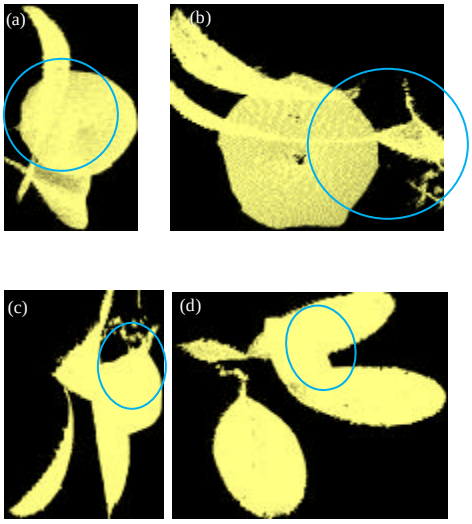

Fig. 6(a-b): Part of the original point clouds of apple, (a) Bottom, (b) Top, (c) Side1 and (d) side7

- Popup splat P_k from S
- Seek the 8-connected neighbor splats (Gross and Pfister, 2007) P_i around P_k in xyz directions by Euclidean distance of $\hat{p}_k$ and $\hat{p}_i$, with $Flag_i = 0$ (Wang *et al*., 2006)

For each P_i, the dot product of normals in Eq. 12 and surface variance difference in Eq. 13 are used as geometric similarity $||P_i-P_k||$ of all leaves and the apple:

$$|n_j \cdot n_k| > \mu \quad (12)$$

$$|c_i - c_k| > \varepsilon \quad (13)$$

When geometric similarity are satisfied and $flag_i = 0$ push P_i to stack S, set $flag_i$ and store $flag_i = 1$ to Oct (splat), else, return to step iii for next P_i.

This iteration will stop until stack S is empty, as shown in Fig. 5b.

MAIN RESULTS

In this study, the point clouds of apple are sampled by 3D CaMega PCP-400 from 11 angles, of which, 1 range scan is bottom face, 1 is top face and 9 are side faces. These faces are managed in Eq. 14:

$$app(11) = \{b, t, s_1, s_2, s_3, s_4, s_5, s_6, s_7, s_8, s_9\}$$

The spatial resolution of point clouds is 0.03mm, the point numbers corresponding to app (11) are {134, 642; 124, 562; 107, 619; 94, 843; 97, 081; 96, 882; 90, 585; 97, 564; 95, 135; 98, 108; 92, 493} respectively and the part of original point clouds is shown in Fig. 6, those parts circled by blue color is "pure" apple faces.

Simplification: In the iterative simplification, threshold k and normals consistency parameter δ in Eq. 5 are the key parameters for subdivision. The larger k value and smaller δ value will result in inadequate segmentation, while the smaller k value and larger δ value will result in over-segmentation, which make calculation complexity increase by geometrical progression. In the following, appropriate k and δ in Eq. 5 are searched by experiment from k = 20, 25, 30 and δ = 1, 0.95, 0.90. The linear correlation coefficient in (15) is employed for quantitative analysis between two point sets of k = 30 and k = 30, δ = 1.

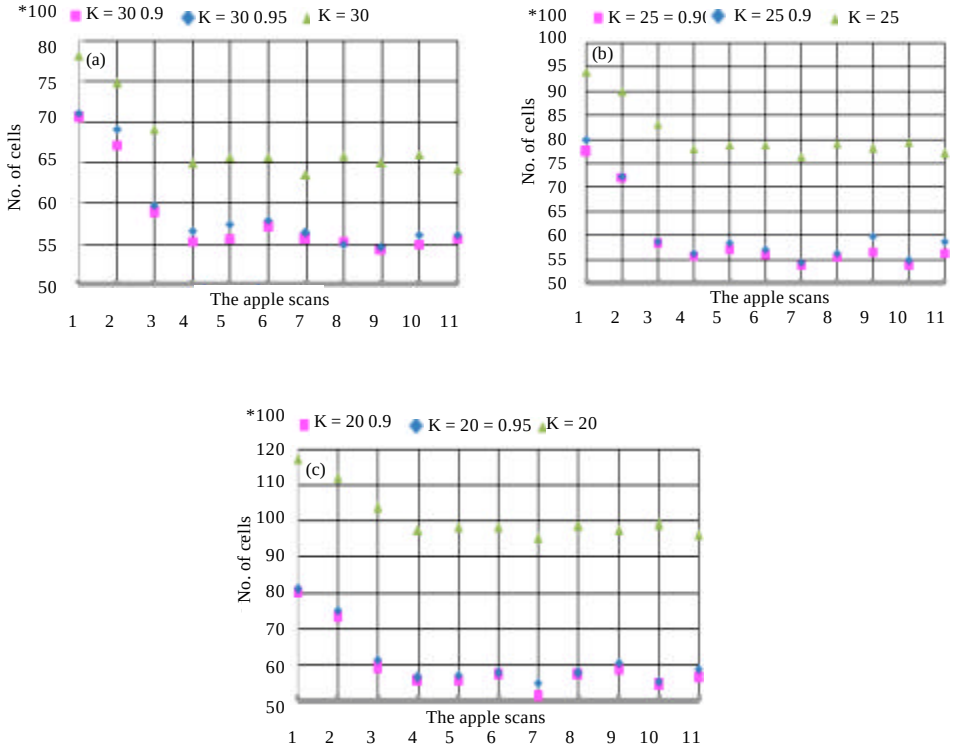

Fig. 7(a-c): Effect of δ on the num of apple cells for different k-value, (a) Num of cells for 3 kinds of δ when k = 30, (b) Num of cells for 3 kinds of δ when k = 25 and (c) Num of cells for 3 kinds of δ when k = 20

For apple scans, the correlation coefficient r = 0.9329, i.e. the two point sets are replaceable. Then, appropriate k and δ value will be specified by next two steps.

First step, for each fixed k, when δ is 1.0, 0.95, 0.9, the number of segmentation units for apple is shown in Fig. 7. From the Fig. 7, we have the following conclusion:

- **Corollary3.1:** Any value for k, the number of cells is the most when δ = 1
- **Corollary3.2:** Any value for k, the number of segmented cells is greatly reduced when δ = 0.95, i.e., 0.95 has an important impact on the segmentation process, which make flat surface segmentation more reasonable due to taking the curvature into account
- **Corollary3.3:** Correlation coefficient r between δ = 0.95 and δ = 0.9 of three group data for k = 30, 25, 20 is respectively 0.993629, 0.992075, 0.994559, i.e. 0.9 is insignificance in the segmentation process

So, for any k, δ = 0.95 is the most appropriate.

Second step, for each fixed δ, when k is 20, 25, 30, the number of segmentation cells is shown in Fig. 8. From Fig. 8, we have the following conclusion:

- **Corollary3.1.** Figure 8a illustrates, only k-neighbor segmentation will result in inadequate segmentation or over-segmentation
- **Corollary3.2.:** Any value for δ, k = 30 will result in inadequate segmentation; k = 20 will result in over-segmentation and complex iterative process
- **Corollary3.3:** Correlation coefficient r between k = 25 and k = 20 of two groups data for δ = 0.95, 0.9 is respectively 0.991449, 0.972537, i.e. k = 25 make the segmentation process more simple and should be appropriate

Finally, the two step experiments analysis indicates, δ = 0.95, k = 25 is the best parameters group.

Local fitting: In MLS fitting, the Gaussian parameter pa in Eq. 8 is set to 0.3 and then some properties of

Table 1: Contrast on number of cells between unextracted and extracted apple scans

Scanns	Bottom	Top	Side 1	Side 2	Side 3	Side 4	Side 5	Side 6	Side 7	Side 8	Side 9
Unextracted	7978.0	7213.0	5855.0	5611.0	5841.0	5694.0	5428.0	5611.0	5963.0	5468.0	5867.0
Extracted	4578.0	4001.0	3035.0	2731.0	2877.0	2802.0	2580.0	2770.0	2907.0	2708.0	2819.0
Decrease ratio/£¥	42.6	44.5	48.2	51.3	50.7	50.8	52.5	50.6	51.2	50.5	51.9

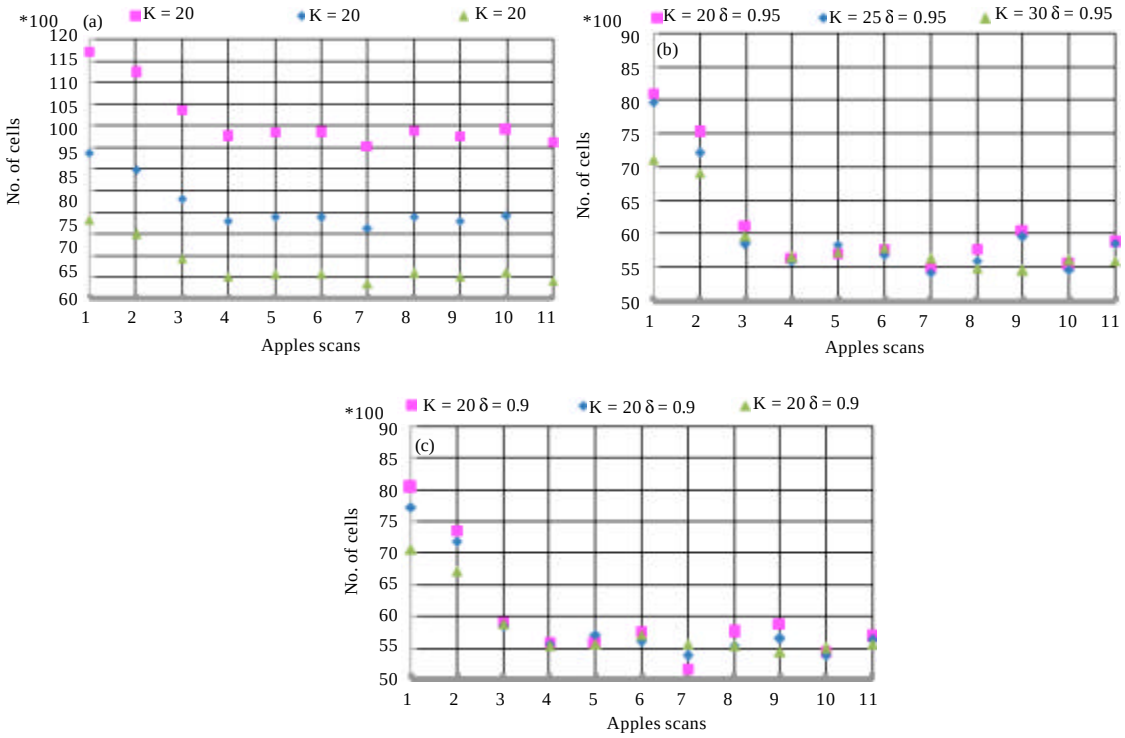

Fig. 8(a-c): Effect of k-value on the num of apple cells for different δ-value (a) Num of cells for 3 kinds of k-value without δ, (b) Num of cells for 3 kinds of k-value when δ = 0.95 and (c) Num of cells for 3 kinds of k when δ = 0.9

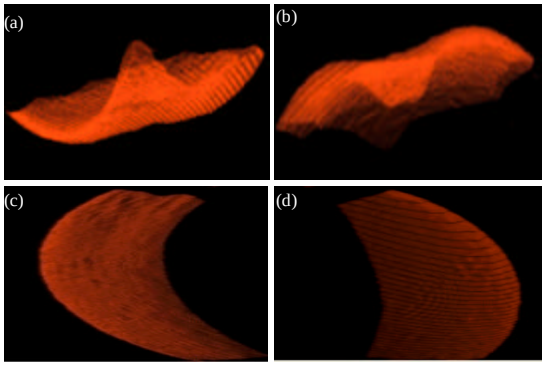

Fig. 9(a-d): Ultimate segmented apple, (a) Bottom, (b) Top, (c) Side1 and (d) Dide7

splat are calculated in this simulation. Next, curvature is estimated for the final extraction.

From Fig. 7b and 8b, the improved K-neighborhood help to reduce the number of cells of apple scans to 3.0% of the original points, a 25% drop than the pure K-neighborhood (4%).

Extraction result: The extraction experiment simulation shows that, parameters for dot product of normals $\mu = 0.95$ in Eq. 12 and surface variance difference $\varepsilon = 0.025$ in Eq. 13 are feasible for identifying apple splats from leaves. Part of the ultimate extracted apple scans are shown in Fig. 9.

After extraction, the number of splats declines obviously, contrast on number between before and after extraction is presented in Table 1. After extraction, the number of average splats decreased by 49.5% than that of before extraction.

CONCLUSION

For quickly and accurately extraction of the apple shape from clutter background, a K-neighborhood based adaptive octree subdivision was first employed for simplifying the point cloud while preserving ability on detail representation and MLS-based local fitting has solved "gap" problem among splats. GSA-based recursive extraction algorithm has avoided processing the leaves and tree trunks, which minimized number of processed splats and speed up the extraction process. Experiments show that the simplification algorithm has made the apple cells drop to 3.0%, which reduced 25% than K-neighborhood simplification, the number of extracted splats decreased by 49.5% than that before extraction. It can be extended to extract other fruits shape with smooth surface. However, this work only can be used for smooth surface extraction and the key parameters were obtained by orthogonal extraction experiments only for apple surfaces, it remained to searching for more theoretical foundation.

ACKNOWLEDGMENT

This study was financially supported by the National High Technology Research and Development Program of China (863 Program, No. 2013AA10230402), China National Undergraduates Innovating Experimentation Project (No.1210712124), the National High Technology Research and Development Program of China (2011BAD21B05) and Chinese Universities Scientific Fund (QN2011036).

REFERENCES

Colombo, C., D. Comanducci and A.D. Bimbo, 2006. A desktop 3D scanner exploiting rotation and visual rectification of laser profiles. Proceedings of the IEEE International Conference on Computer Vision Systems, January 4-7, 2006, New York, USA., pp: 49-54.

Dong, Q.X., Y.M. Wang, J.F. Barczi, P. De Reffye and J.L. Hou, 2003. Tomato growth modeling based on interaction of its structure-function. Proceedings of the International Symposium on Plant Growth Modeling, Simulation, Visualization and their Applications, October 13-16, 2003, Beijing, China, pp: 250-262.

Gross, M. and H. Pfister, 2007. Point-Based Graphics. 1st Edn., Morgan Kaufmann Publishers, USA., ISBN: 978-0123706041, Pages: 552.

Iskurt, A. and Y. Becerikli, 2010. Fast and automatic Brain Extraction by Geodesic Passive Contours (BEGPC). Int. J. Innovative Comput. Inform. Control, 6: 5665-5684.

Jancsok, P.T., L. Clijmans, B.M. Nicola and J. De Baerdemaeker, 2001. Investigation of the effect of shape on the acoustic response of conference pears by finite element modeling. Postharvest Biol. Technol., 29: 1-12.

Levin, D., 2003. Mesh-Independent Surface Interpolation. In: Geometric Modeling for Scientific Visualization, Brunnett, G., B. Hamann, H. Muller and L. Linsen (Eds.). Springer, USA., pp: 37-49.

Marin, P., A. Meyer and V. Guigue, 2001. Partition along characteristic edges of a digitized point cloud. Proceedings of the International Conference on Shape Modeling and Applications, May 7-11, 2001, Genova, Italy, pp: 326-334.

Nan, L., A. Sharf, A. Zhang, H. Zhang, D. Cohen-Or and B. Chen, 2010. SmartBoxes for interactive urban reconstruction. Proceedings of the 37th International Conference and Exhibition on Computer Graphics and Interactive Techniques, July 26-30, 2010, Los Angeles, CA., USA.

Pang, X.F. and M.Y. Pang, 2009. An algorithm for extracting geometric features from point cloud. Proceedings of the International Conference on Information Management, Innovation Management and Industrial Engineering, December 26-27, 2009, Xian, China, pp: 78-83.

Uyar, R. and F. Erdogdu, 2009. Potential use of 3-dimensional scanners for food process modeling. J. Food Eng., 93: 337-343.

Vincent, G. and G. Harja, 2008. Exploring ecological significance of tree crown plasticity through three-dimensional modelling. Ann. Bot., 101: 1221-1231.

Wang, S.D., Y. Chen, B.F. Zhang, G.L. Sun and X.M. Huang, 2006. The application of octrees in 3D modeling. J. Anhui Inst. Archit. Ind., 14: 96-98.

Wu, J., Z. Zhang and L. Kobbelt, 2005. Progressive Splatting. In: Advances in Multiresolution for Geometric Modelling (Mathematics and Visualization), Dodgson, N., M.S. Floater and M. Sabin (Eds.). Springer, USA., pp: 147-170.

Wu, L.F. and X.L. Meng, 2008. A robust object segmentation method. Int. J. Innovative Comput. Inform. Control, 4: 3059-3066.

Zhou, C.J., X.P. Wei, Q. Zhang and B.X. Xiao, 2008. Image reconstruction for face recognition based on fast ICA. Int. J. Innovative Comput. Inform. Control, 4: 1723-1732.